Electronic Supplementary Information

Tetrahydro[5]helicene-based imide dyes with intense fluorescence in both solution and solid state

Meng Li,[a,c] Yingli Niu,[b] Xiaozhang Zhu,[b] Qian Peng,[b] Hai-Yan Lu,[c,*] Andong Xia[b,*] and Chuan-Feng Chen[a,*]

[a]*Beijing National Laboratory for Molecular Sciences, CAS Key Laboratory of Molecular Recognition and Function, Institute of Chemistry, Chinese Academy of Sciences, Beijing 100190, China. Fax: 8610-62554449; E-mail: cchen@iccas.ac.cn*

[b]*Institute of Chemistry, Chinese Academy of Sciences, Beijing 100190, China. Email: andong@iccas.ac.cn*

[c]*University of Chinese Academy of Sciences, Beijing 100049, China. Email: haiyanlu@ucas.ac.cn*

1. General Information

All reactants were commercial and used without further purification excepted as noted. Melting points are uncorrected. ^{1}H NMR and ^{13}C NMR spectra were recorded with a DMX300 NMR at 298 K. MALDI-TOF mass spectra were determined with a BIFLEXIII mass spectrometer. HRMS mass spectra were measured in the ESI mode. The single crystal data of **3** was collected on Rigaku Saturn diffractometer with CCD area detector. All calculations were performed using the SHELXL97 and crystal structure crystallographic software packages. Absolute fluorescence quantum yields were measured by Hamamatsu Photonics Quantaurus QY at room temperature. Fluorescence lifetimes were measured based on the time resolved PL experiments.

The quantum yields of **3** and **5** are theoretically studied. The molecular fluorescence quantum yield η is defined as $\eta = k_r / (k_r + k_{nr})$, where k_r and k_{nr} are the molecular radiative (emission) and non-radiative rates. The main contribution to k_{nr} comes from internal conversion (IC) process.[1] We calculated the radiative rate k_r and IC rate k_{ic} applying the "thermal vibration correlation function" method.[2-5] The quantum chemistry calculations of **3** and **5** were carried out with the TURBOMOLE 6.4 program package.[6] The geometries of the ground and excited stateswere optimized with density functional theory (DFT)[7] andtime-dependent density functional theory (TDDFT),[8] respectively. The B3LYP functional[9, 10] and 6-31G** basis sets[11, 12] were used. Then the normal modes and frequencies of the ground and excited states and nonadiabatic coupling matrix elements (NACMEs) were calculated. The correlation function of absorption, emission, and IC were calculated with home-built programs. The Fourier transformation of the correlation functions were carried out with the FFT routines of the FFTW LIBRARY (version 3.1.2).

1. S. H. Lin, *J. Chem. Phys.*, 1966, **44**, 3759-3767.

2. Y. Niu, Q. Peng, C. Deng, X. Gao and Z. Shuai, *J. Phys. Chem. A*, 2010, **114**, 7817-7831.

3. Y. Niu, Q. Peng and Z. Shuai, *Sci. China Ser. B-Chem.*, 2008, **51**, 1153-1158.

4. Q. Peng, Y. Yi, Z. Shuai and J. Shao, *J. Chem. Phys.*, 2007, **126**, 114302.

5. Q. Peng, Y. Yi, Z. Shuai and J. Shao, *J. Am. Chem. Soc.*, 2007, **129**, 9333-9339.

6. TURBOMOLE V6.4 2012, a development of University of Karlsruhe and Forschungszentrum Karlsruhe GmbH, 1989-2007, TURBOMOLE GmbH, since 2007; available from http://www.turbomole.com.

7. O. Treutler and R. Ahlrichs, *J. Chem. Phys.*, 1995, **102**, 346-354.

8. F. Furche and R. Ahlrichs, *J. Chem. Phys.*, 2002, **117**, 7433-7447.

9. A. D. Becke, *J. Chem. Phys.*, 1993, **98**, 5648-5652.

10. P. J. Stephens, F. J. Devlin, C. F. Chabalowski and M. J. Frisch, *J. Phys. Chem.*, 1994, **98**, 11623-11627.

11. W. J. Hehre, R. Ditchfield and J. A. Pople, *J. Chem. Phys.*, 1972, **56**, 2257-2261.

12. P. C. Hariharan and J. A. Pople, *Theoret. chim. Acta (Berl.)*, 1973, **28**, 213-222

13. J. R. Reimers *J. Chem. Phys*., 2001, **115**, 9103-9109.

2. Experimental procedures and characterization of new compounds

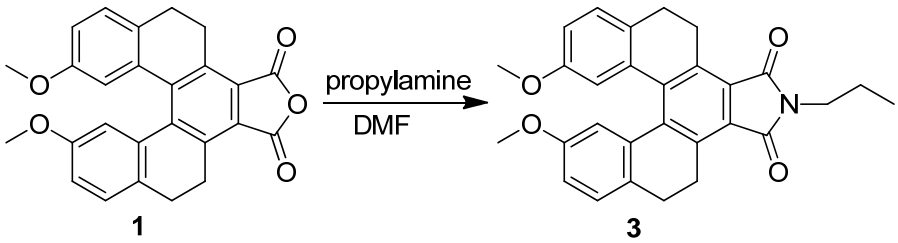

1 **3**

Compound 3. A mixtrue of **1** (412 mg, 1 mmol) and *n*-propylamine (295 mg, 5 mmol) in DMF (20 mL) was heated at 70 °C for 24 hours. After cooled to room temperature, ethyl acetate (40 mL) was added. The organic phase was washed with saturated brine (3×20 mL), dried over anhydrous $MgSO_4$. The solvent was removed in *vacuo*, and the residue was submitted to column chromatography with

ethyl acetate and petroleum ether (1:5,v/v, R_f = 0.48) as eluent to give **3** (326 mg, 72%) as yellow solid. m. p.: 178-179°C. ^{1}H NMR (300 MHz, $CDCl_3$): δ 7.21 (d, *J* = 8.2 Hz, 2H), 6.76 (dd, *J* = 8.2, 2.6 Hz, 2H), 6.71 (d, *J* = 2.5 Hz, 2H), 4.13–4.07 (m, 2H), 3.64 (dd, *J* = 7.5, 5.6 Hz, 2H), 3.42 (s, 6H), 2.91–2.75 (m, 4H), 2.59–2.38 (m, 2H), 1.78–1.65 (m, 2H), 0.97 (t, *J* = 7.4 Hz, 3H). ^{13}C NMR (75 MHz, $CDCl_3$): δ 169.2, 157.5, 138.8, 138.7, 134.1, 131.8, 128.8, 126.2, 115.5, 115.3, 55.2, 39.5, 27.8, 24.6, 22.1, 11.5. MALDI-TOF MS: *m/z* 454.1 $[M+H]^+$. HRMS (ESI): *m/z* calcd for $C_{29}H_{28}NO_4$ $[M + H]^+$ 454.2013, found 454.2018.

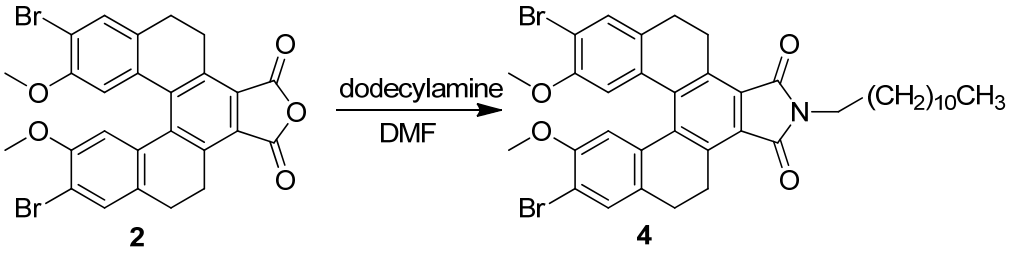

2 **4**

Compound 4. A mixtrue of **2** (11.4 g, 20 mmol) and *n*-dodecyl amine (9.25 g, 50 mmol) in DMF (100 mL) was heated at 100 °C for 24 hours. After cooled to room temperature, ethyl acetate (200 mL) was added. The organic phase was washed with saturated brine (3×100 mL), dried over anhydrous $MgSO_4$. The solvent was removed in *vacuo* and the residue was submitted to column chromatography with ethyl acetate and petroleum ether (1:5,v/v, R_f = 0.67) as eluent to give **4** (11.37 g, 77%) as yellow solid. m. p.: 75-76 °C. ^{1}H NMR (300 MHz, $CDCl_3$): δ 7.52 (s, 2H), 6.66 (s, 2H), 4.14–4.09 (m, 2H), 3.69–3.64 (m, 2H), 3.38 (s, 6H), 2.90–2.73 (m, 4H), 2.55–2.43 (m, 2H), 1.74–1.60 (m, 2H), 1.38–1.21 (m, 18H), 0.87 (t, *J* = 6.6 Hz, 3H). ^{13}C NMR (75 MHz, $CDCl_3$): δ 168.8, 153.8, 138.4, 137.9, 133.2, 133.1, 132.6, 126.6, 114.5, 112.0, 56.0, 38.0, 32.0, 29.74, 29.71, 29.6, 29.5, 29.4, 28.7, 27.4, 27.0, 24.2, 22.8, 14.2. MALDI-TOF MS: *m/z* 738.2 $[M]^+$. HRMS (ESI): *m/z* calcd for $C_{38}H_{44}Br_2NO_4$ $[M + H]^+$ 736.1632, found 736.1623.

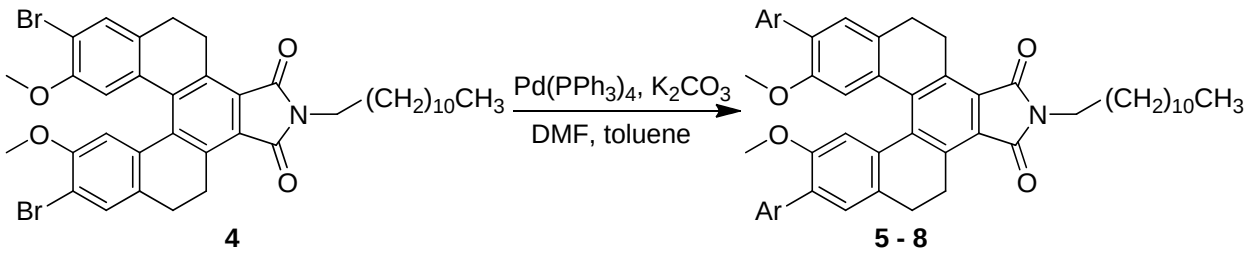

4 **5 - 8**

General procedure of Suzuki-Miyaura cross coupling:

To a mixture of compound **4** (700 mg, 0.95 mmol) , K_2CO_3 (1.31 g, 9.9 mmol), and arylboronic acid (2.85 mmol) in DMF (30 mL) and toluene (20 mL) under argon atmosphere was added catalytic amount of $Pd(PPh_3)_4$ (5% mol). The resulting mixture was stirred for 12 hours at 90°C under argon atmosphere, cooled to room temperature and then poured into ethyl acetate (100 mL). The organic layer was washed with saturated brine (3×100 mL), dried over anhydrous $MgSO_4$ and then concentrated in *vacuo*. The residue was purified by column chromatography with ethyl acetate and petroleum ether (1:5, v/v) as eluent to give the pure product.

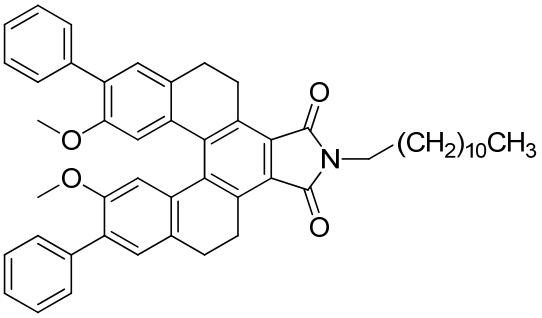

Compound 5. According to the general method, **5** (639 mg, 92%) was obtained (R_f = 0.71) as yellow powder. m. p.: 120-121 °C. ^{1}H NMR (300 MHz, $CDCl_3$): δ 7.56–7.49 (m, 4H), 7.44–7.38 (m, 4H), 7.37–7.27 (m, 4H), 6.86 (s, 2H), 4.19–4.14 (m, 2H), 3.74–3.63 (m, 2H), 3.33 (s, 6H), 2.97–2.82 (m, 4H), 2.64–2.51 (m, 2H), 1.75–1.64 (m, 2H), 1.34–1.26 (m, 18H), 0.88 (t, *J* = 6.7 Hz, 3H). ^{13}C NMR (75 MHz, $CDCl_3$): δ 169.2, 154.2, 138.7, 138.4, 138.0, 133.2, 132.0, 130.9, 130.1, 129.4, 128.3, 127.4, 126.3, 114.1, 55.3, 38.0, 32.1, 29.77, 29.75, 29.66, 29.5, 29.4, 28.8, 27.7, 27.1, 24.5,

22.8, 14.3. MALDI-TOF MS: *m/z* 731.4 $[M]^+$. HRMS (ESI): *m/z* calcd for $C_{50}H_{54}NO_4$ $[M + H]^+$ 732.4047, found 732.4038.

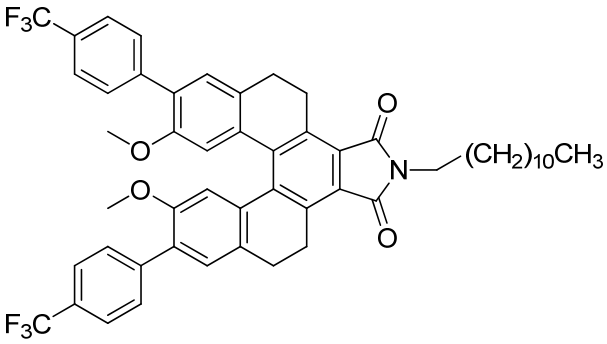

Compound 6. According to the general method, **6** (577 mg, 70%) was obtained (R_f = 0.61) as yellow powder. m. p.: 160-161 °C. ^{1}H NMR (300 MHz, $CDCl_3$): δ 7.69–7.61 (m, 8H), 7.30 (s, 2H), 6.86 (s, 2H), 4.21–4.16 (m, 2H), 3.72–3.66 (m, 2H), 3.33 (s, 6H), 2.98–2.83 (m, 4H), 2.64–2.52 (m, 2H), 1.76–1.63 (m, 2H), 1.34–1.26 (m, 18H), 0.88 (t, *J* = 6.7 Hz, 3H). ^{13}C NMR (75 MHz, $CDCl_3$): δ 169.0, 154.2, 141.5, 138.7, 138.3, 134.0, 132.3, 130.1, 129.7, 129.4, 129.2, 126.5, 125.2, 125.14, 125.10, 114.1, 55.3, 38.1, 32.1, 29.8, 29.74, 29.66, 29.5, 29.4, 28.8, 27.7, 27.1, 24.4, 22.8, 14.3. MALDI-TOF MS: *m/z* 867.2 $[M]^+$. HRMS (ESI): *m/z* calcd for $C_{52}H_{52}NO_4F_6$ $[M + H]^+$ 868.3795, found 868.3786.

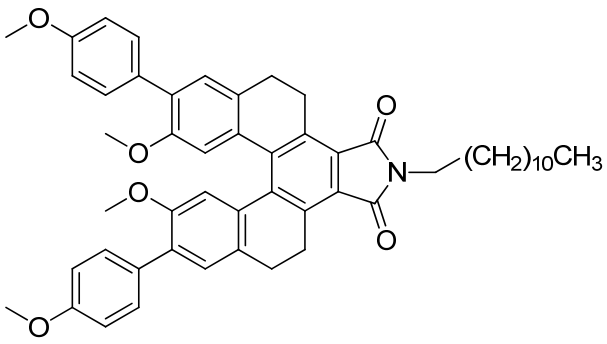

Compound 7. According to the general method, **7** (676 mg, 90%) was obtained (R_f = 0.43) as yellow powder. m. p.: 97-99 °C. ^{1}H NMR (300 MHz, $CDCl_3$): δ 7.49–7.46 (m, 4H), 7.26 (s, 2H), 6.96–6.93 (m, 4H), 6.85 (s, 2H), 4.18–4.13 (m, 2H), 3.85 (s, 6H), 3.70–3.66 (m, 2H), 3.32 (s, 6H),

2.97–2.81 (m, 4H), 2.64–2.48 (m, 2H), 1.76–1.62 (m, 2H), 1.34–1.26 (m, 18H), 0.87 (t, J = 6.6 Hz, 3H). ^{13}C NMR (75 MHz, $CDCl_3$): δ 169.2, 159.1, 154.2, 138.7, 138.4, 132.8, 132.1, 130.6, 130.5, 130.3, 129.8, 126.2, 114.0, 113.8, 55.5, 55.3, 38.0, 32.1, 29.78, 29.77, 29.75, 29.66, 29.5, 29.4, 28.8, 27.7, 27.1, 24.5, 22.8, 14.3. MALDI-TOF MS: *m/z* 791.5 $[M]^+$. HRMS (ESI): *m/z* calcd for $C_{52}H_{58}NO_6$ $[M + H]^+$ 792.4259, found 792.4253.

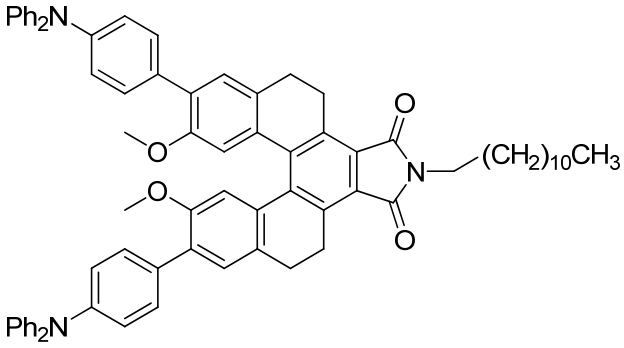

Compound 8. According to the general method, **8** (791 mg, 78%) was obtained (R_f = 0.56) as yellow powder. m. p.: 120-122°C. ^{1}H NMR (300 MHz, $CDCl_3$): δ 7.43 (d, J = 8.6 Hz, 4H), 7.31–7.22 (m, 10H), 7.17–6.99 (m, 16H), 6.86 (s, 2H), 4.15 (d, J = 15.9 Hz, 2H), 3.70–3.65 (m, 2H), 3.33 (s, 6H), 3.02–2.76 (m, 4H), 2.67–2.46 (m, 2H), 1.77–1.62 (m, 2H), 1.34–1.26 (m, 18H), 0.87 (t, J = 6.5 Hz, 3H). ^{13}C NMR (75 MHz, $CDCl_3$): δ 169.2, 154.3, 147.8, 147.1, 138.7, 138.5, 132.9, 132.1, 131.8, 130.4, 130.2, 129.8, 129.4, 126.2, 124.7, 123.2, 123.1, 114.1, 55.3, 38.0, 32.1, 29.8, 29.74, 29.65, 29.5, 29.4, 28.8, 27.8, 27.1, 24.5, 22.8, 14.2. MALDI-TOF MS: *m/z*1066.7 $[M+H]^+$. HRMS (ESI): *m/z* calcd for $C_{74}H_{72}N_3O_4$ $[M + H]^+$ 1066.5517, found 1066.5509.

3. X-ray crystallographic data and packing structure

Table S1. X-ray crystallographic data of **3**

Name	**3**
Empirical formula	$C_{29}H_{27}NO_4$
Formula weight	453.52
Temperature	173(2) K
Crystal system	Monoclinic
Space group	P2(1)/n
a, Å	15.388(6)
b, Å	6.680(3)
c, Å	22.363(9)
alpha, deg	90
beta, deg	93.69(3)
gamma, deg	90
Volume, $Å^3$	2293.9(16)
Z	4
Calculated density, Mg/m^3	1.313
Absorption coefficient, mm^{-1}	0.087
F(000)	960
Crystal size, mm	0.71 x 0.65 x 0.36
Theta range for data collection, deg	3.12 to 27.50
Limiting indices	-19<=h<=19,-8<=k<=8,-28<=l<=28
Reflections collected / unique	16753 / 5220 [R(int) = 0.0436]
Completeness to theta = 27.49	99.0 %
Absorption correction	Semi-empirical from equivalents
Max. and min. transmission	1.0000 and 0.5317
Refinement method	Full-matrix least-squares on F^2
Data / restraints / parameters	5220 / 0 / 310
Goodness-of-fit on F^2	1.169
Final R indices [I>2sigma(I)]	R1 = 0.0702, wR2 = 0.1671
R indices (all data)	R1 = 0.0753, wR2 = 0.1710
Largest diff. peak and hole, $e.A^{-3}$	0.576 and -0.266

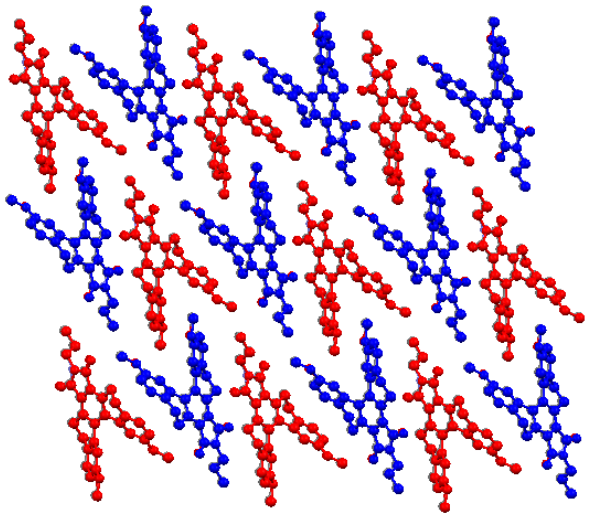

Figure S1. Packing of alternate *M*-helical and *P*-helical configurations of **3** in the racemic crystal structure.

4. Photophysical properties of 3 and 5

Table S2. Photophysical properties of **3** and **5**

Compound	absorption [a]		fluorescence [a]			
	λ_{abs}/nm	logε/M^{-1}cm^{-1}	λ_{em}/nm	Φ_f [b]/%	τ/ns	Stokes shift /nm
3	374	4.30	474	4.9	0.87	100
5	385	4.31	502	70.3	7.53	115

[a]All spectra were recorded in CH_2Cl_2 (c = 1.0 × 10^{-5} M). [b]Absolute fluorescence quantum yield, measured by Hamamatsu Photonics Quantaurus QY. Stokes shift = $\lambda_{em,\,max}-\lambda_{abs,\,max}$

5. Theoretical calculations

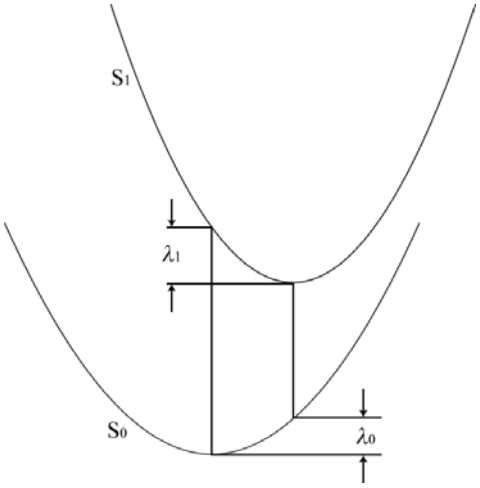

Figure S2. The schematic diagrams of molecular potential energy surfaces S_0 and S_1, and the corresponding reorganization energies λ_0 and λ_1.

The reorganization energies λ_0 and λ_1 can be evaluated either based on adiabatic potential energy surfaces (AP), or approximately from a normal-mode (NM) analysis.[13] λ_0 and λ_1 calculated in both ways were listed in Table S3. The reorganization energy characterizes the geometry relaxation after electronically vertical transition from the equilibrium position. The reorganization λ_0 which related to the emission and IC process from S1, decrease in molecule **5** compared to molecule **3** due to introducing the phenyl groups.

Table S3. The reorganization energy from DFT and TDDFT calculation and projection to the internal coordinates[13]

molecule	AP		NM	
	λ_0 (cm^{-1})	λ_1 (cm^{-1})	λ_0 (cm^{-1})	λ_1 (cm^{-1})
3	1787	1673	1808	1730
5	1670	1747	1678	1772

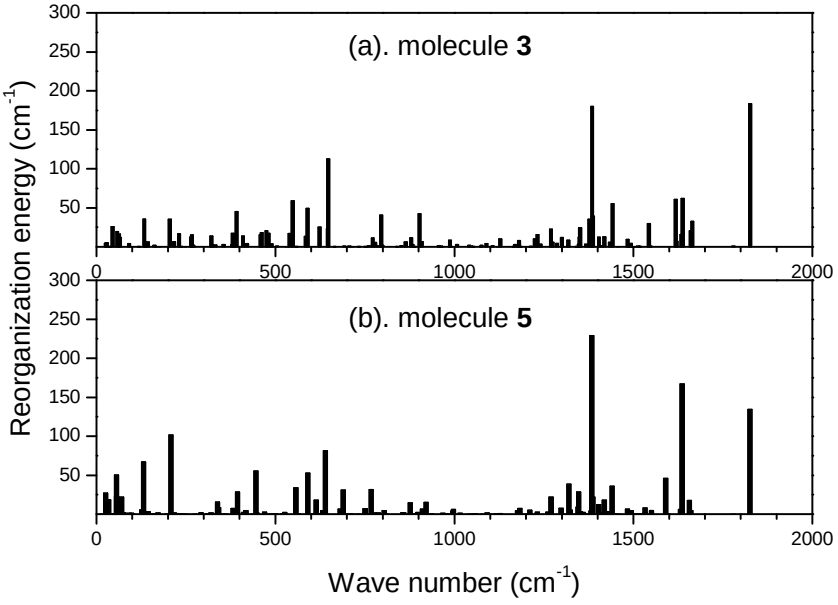

Figure S3. Reorganization energy decomposition in normal modes of molecules **3** (a) and **5** (b).

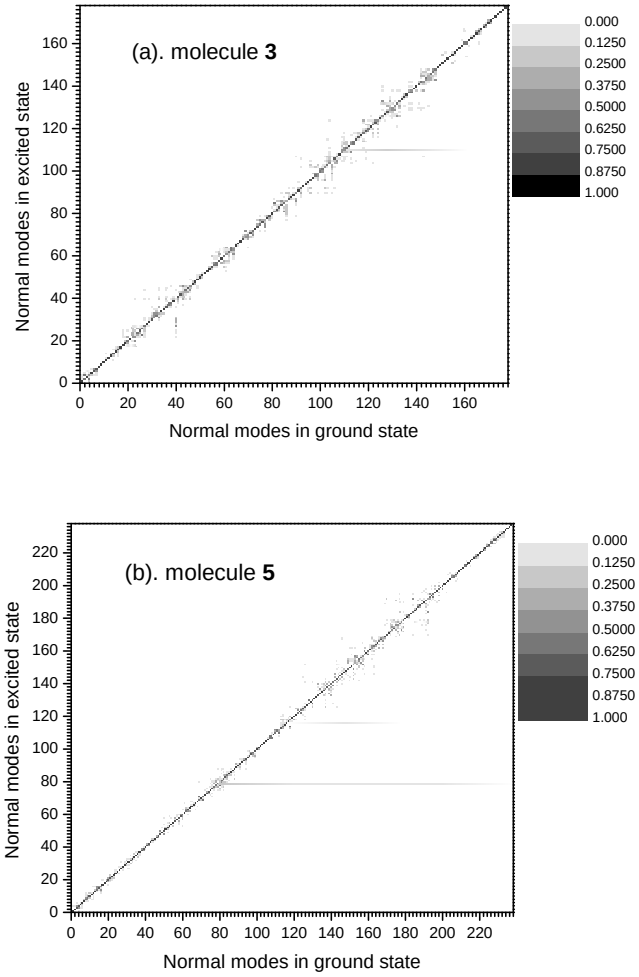

Figure S4. Duschinsky rotation matrix of molecules **3** (a) and **5** (b).

The Duschinsky rotation (mode mixing) matrix **S** and mode displacement **D** defined in Eq. S1 related the normal coordinates $\mathbf{Q}_i$ in the initial electronic state and $\mathbf{Q}_f$ in the final electronic state.In general, the normal mode mixing can broaden the spectra and enhance the IC rate. To assess the mixing level, we define the mixing parameterχ in Eq. S2.χ= 0 means there is no any mixing between initial and final electronic states. Table S4 shows that the mixing parameter χ in molecule **5**is smaller than **3**, which makes the IC rate of 3 (3.13×10^{9} s^{-1}) lower than 5 (4.82×10^{8} s^{-1}).

$$\mathbf{Q}_f = \mathbf{S}\mathbf{Q}_i + \mathbf{D} \tag{S1}$$

$$\chi = 1 - \frac{\sum_{k=1}^{N} |S_{kk}|}{N} \tag{S2}$$

Table S4. The normal mode mixing parameter of molecules **3** and **5**

	molecule **3**	molecule **5**
mixing parameter χ (%)	21.12	16.88

The Fluorescence spectra of **3** and **5** at T=300K are represented in Figure 5. The peaks of the spectra of **3** and **5** in experiment locate at 473nm and 502nm, and in theory the peaks locate at 495nm and 536nm, respectively.

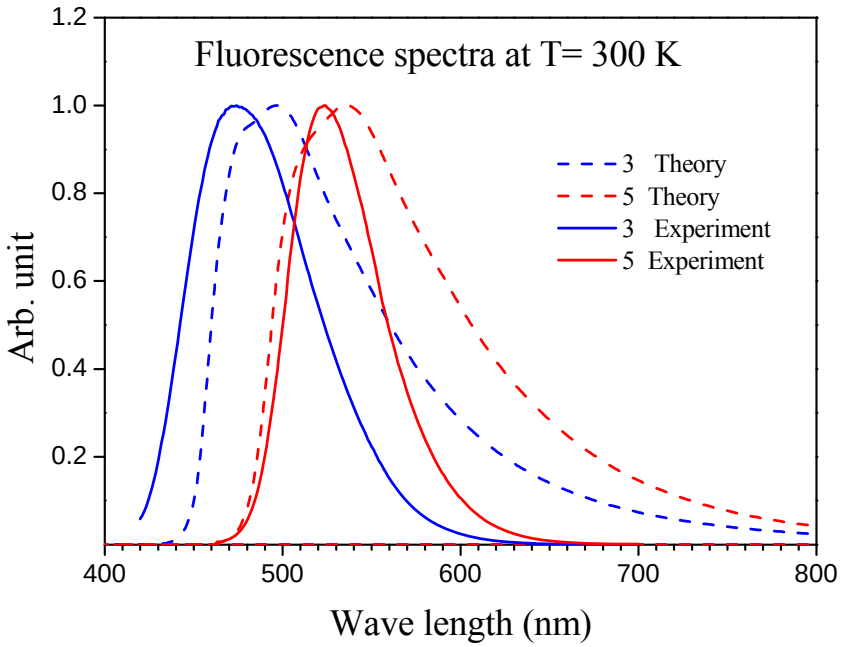

Figure S5. The experimental (solid line) and theoretical (dashed line) fluorescence spectra of **3** and **5** at 300K.

Table S5. The calculated transition dipole moments, emission rates, IC rates and quantum yields of **3** and **5**

compound	μ_f (Debye)	$k_r(s^{-1})$	$k_{ic}(s^{-1})$	Φ_f/%(Theor.)	Φ_f/%(Exp.)
3	3.07	1.74×10^{7}	3.13×10^{9}	0.553	4.9
5	5.12	4.04×10^{7}	4.82×10^{8}	7.73	70.3

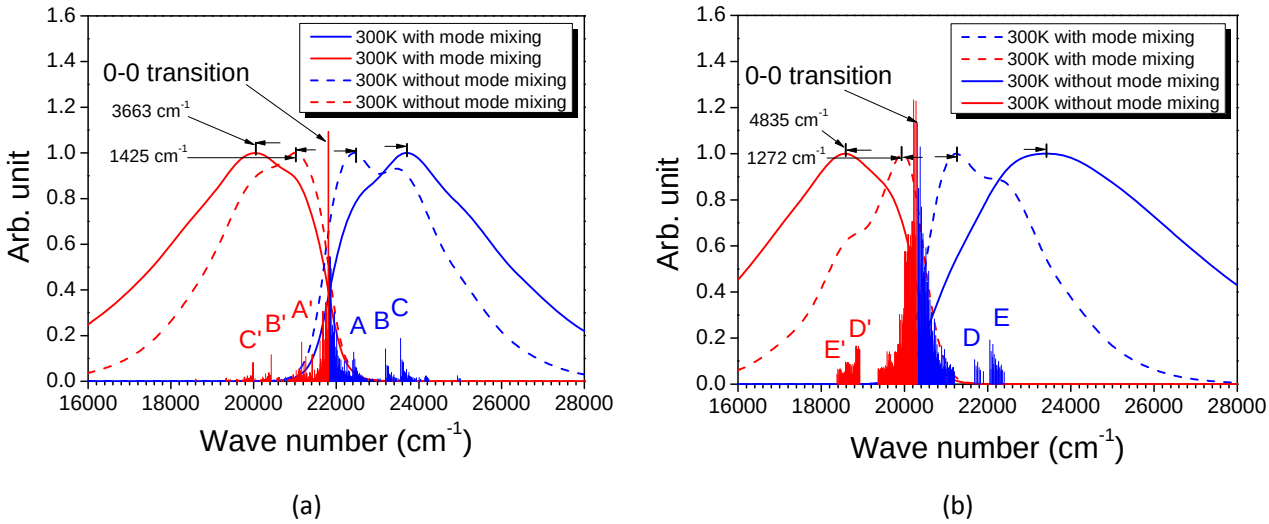

Figure S6. The absorption and fluorescence spectra with (solid line) and without (dashed line) Duschinsky rotation effect (DRE) of molecule **3** (a) and **5** (b) at 300K, respectively.

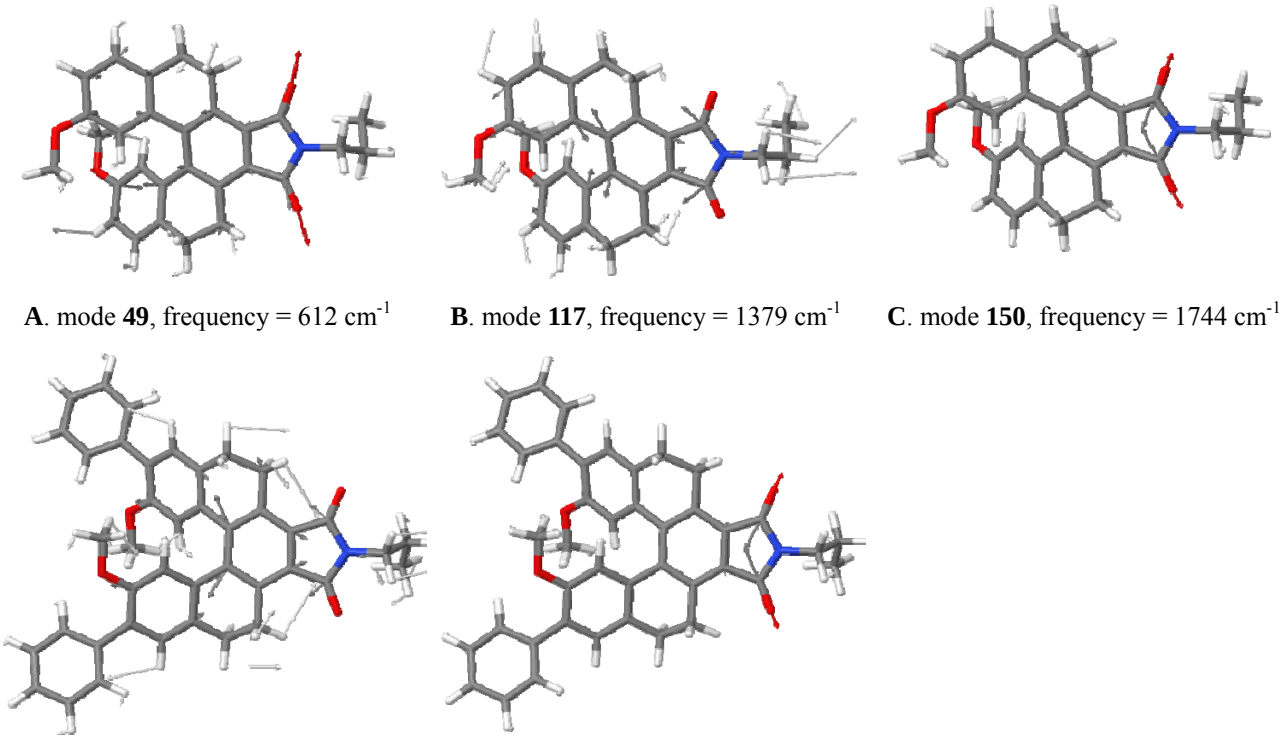

A. mode **49**, frequency = 612 cm^{-1} **B**. mode **117**, frequency = 1379 cm^{-1} **C**. mode **150**, frequency = 1744 cm^{-1}

D. mode **162**, frequency = 1382 cm^{-1} **E**. mode **202**, frequency = 1747 cm^{-1}

Figure S7. The normal mode assigned in the spectra in **Figure S6**.

6. UV/Vis and fluorescence spectra of 5-8

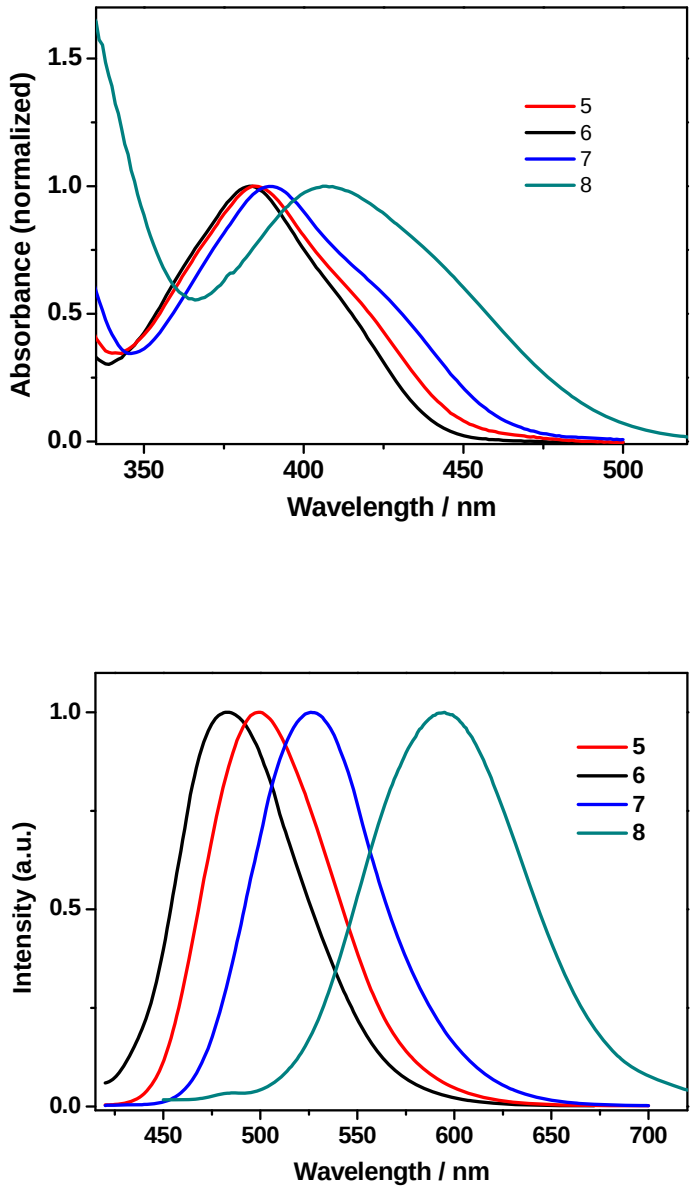

Figure S8. UV/Vis (up) and fluorescence (down) spectra of **5-8** in CH_2Cl_2 at room temperature (c = 1.0×10^{-5} M).

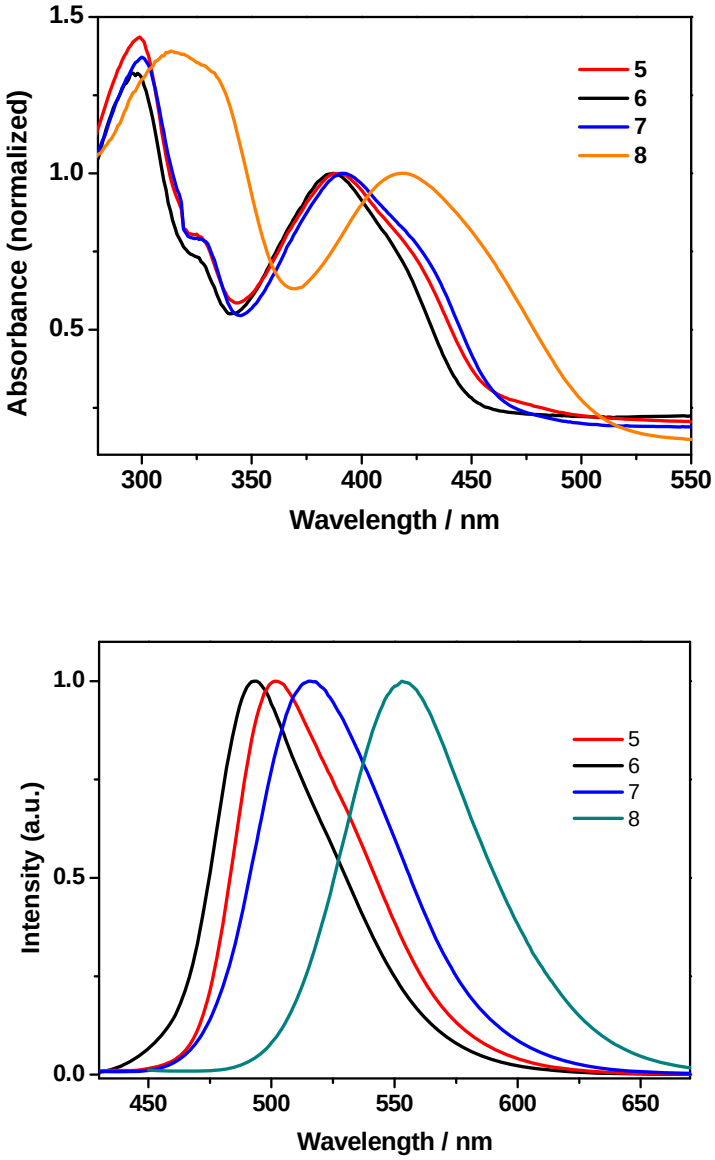

Figure S9. UV/Vis (up) and fluorescence (down) spectra of **5-8** in the solid state (spin-coated film).

Figure S10. The pictures of the spin-coated films of **6**, **5**, **7** and **8** under irradiation of a black light at 365 nm.

7. Photophysical data of 5-8 in various solvents and solid state

Table S6. Photophysical data of **5** in various solvents and in the solid state

	λ_{abs}/nm	λ_{em}/nm	$\Phi_f{}^a$/%
Cyclohexane	380	456	43.5
Toluene	385	474	52.9
Dichoromethane	385	500	70.3
THF	382	483	60.1
Film	390	502	51.0

[a]Absolute fluorescence quantum yield, measured by Hamamatsu Photonics Quantaurus QY

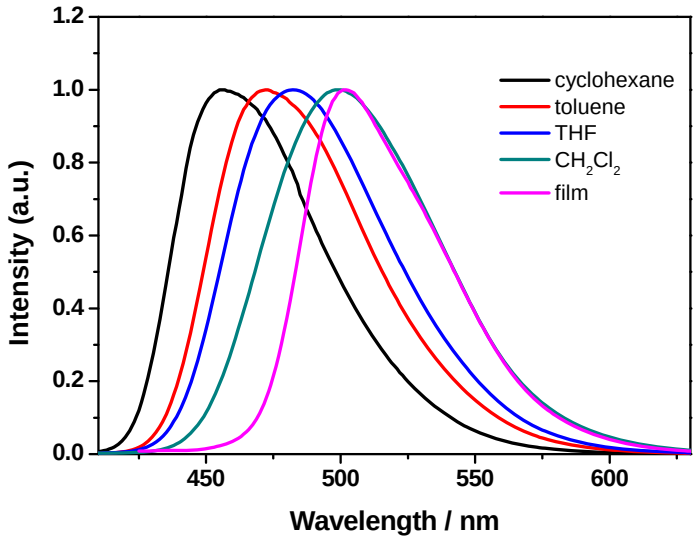

Figure S11.Fluorescence spectra of **5** in various solvents and solid state (spin-coated film).

Table S7. Photophysical data of **6** in various solvents and in the solid state

	λ_{abs}/nm	λ_{em}/nm	$\Phi_f{}^a$/%
Cyclohexane	376	446	39.3
Toluene	385	470	43.9
Dichoromethane	384	483	46.3
THF	381	468	60.8
Film	387	493	50.9

[a]Absolute fluorescence quantum yield, measured by Hamamatsu Photonics Quantaurus QY

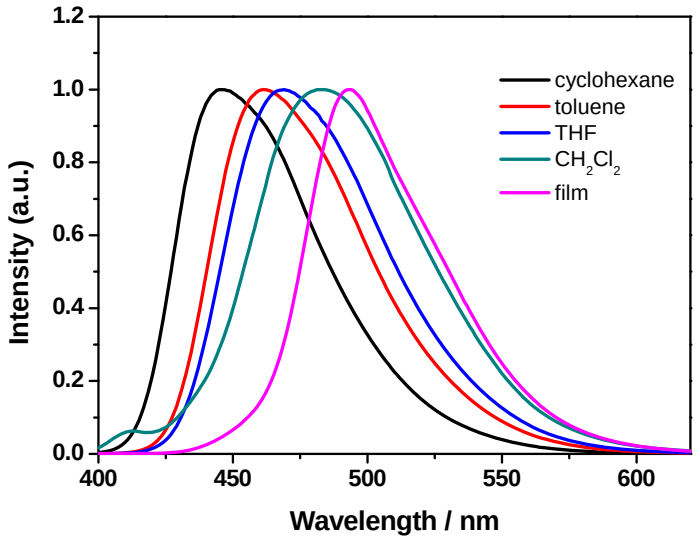

Figure S12. Fluorescence spectra of **6** in various solvents and solid state (spin-coated film).

Table S8. Photophysical data of **7** in various solvents and in the solid state

	λ_{abs}/nm	λ_{em}/nm	Φ_f^a/%
Cyclohexane	385	469	63.7
Toluene	391	491	76.0
Dichoromethane	390	526	85.1
THF	387	506	90.3
Film	394	516	61.8

[a]Absolute fluorescence quantum yield, measured by Hamamatsu Photonics Quantaurus QY

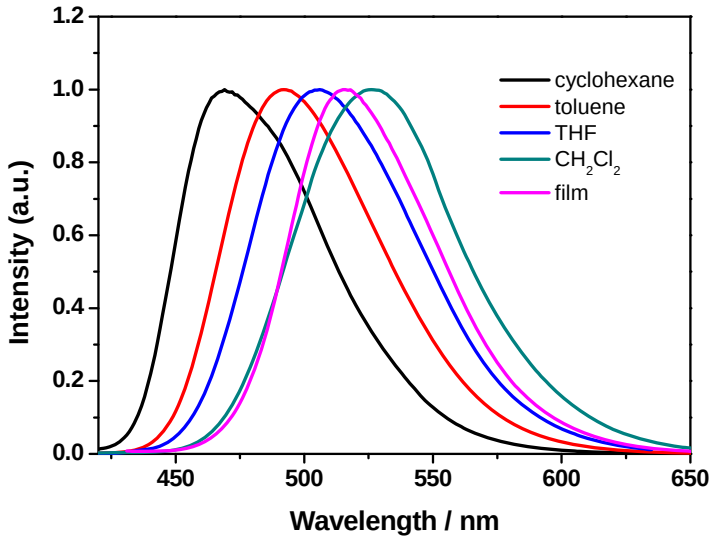

Figure S13. Fluorescence spectra of **7** in various solvents and solid state (spin-coated film).

Table S9. Photophysical data of **8** in various solvents and in the solid state

	λ_{abs}/nm	λ_{em}/nm	$\Phi_f{}^a$/%
Cyclohexane	405	501	76.6
Toluene	411	533	68.5
Dichoromethane	407	595	7.1
THF	404	568	43.9
Film	420	568	67.3

[a]Absolute fluorescence quantum yield, measured by Hamamatsu Photonics Quantaurus QY

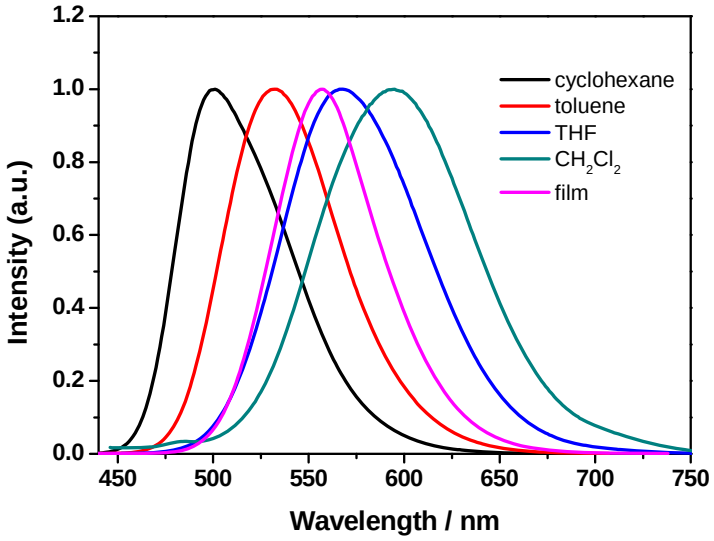

Figure S14. Fluorescence spectra of **8** in various solvents and solid state (spin-coated film).

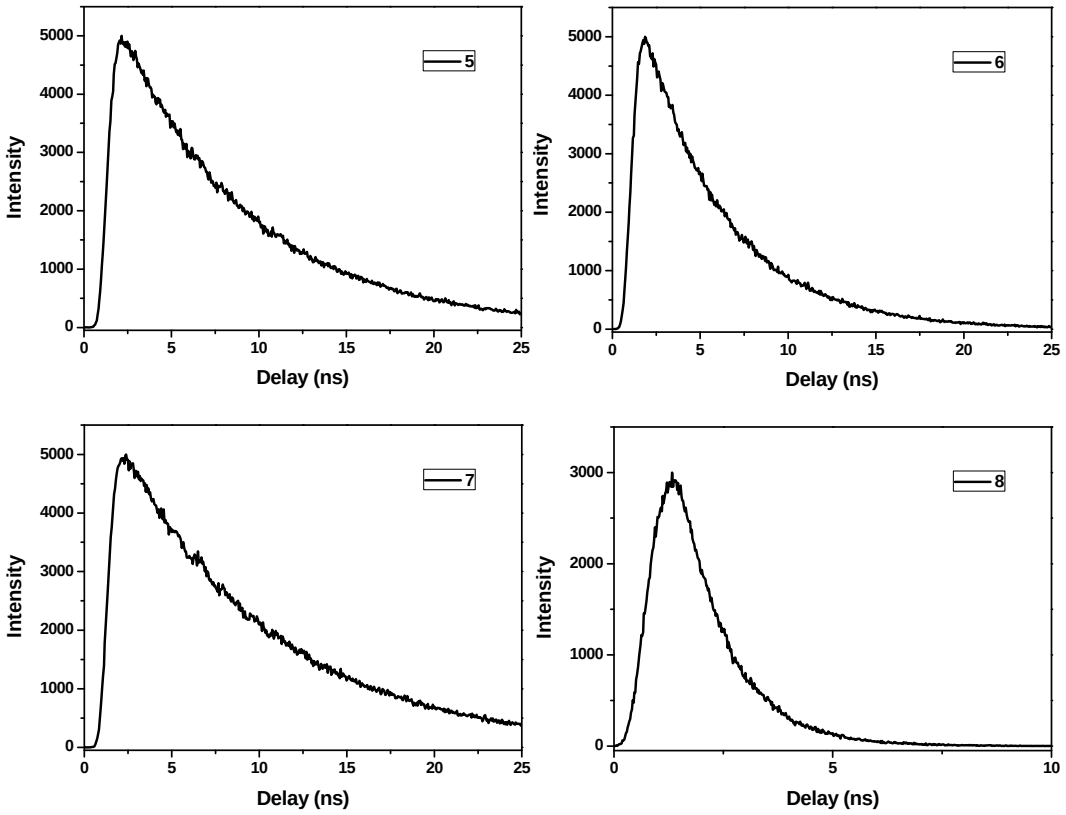

Figure S15. Fluorescence lifetime of **5-8** in CH_2Cl_2 at room temperature.

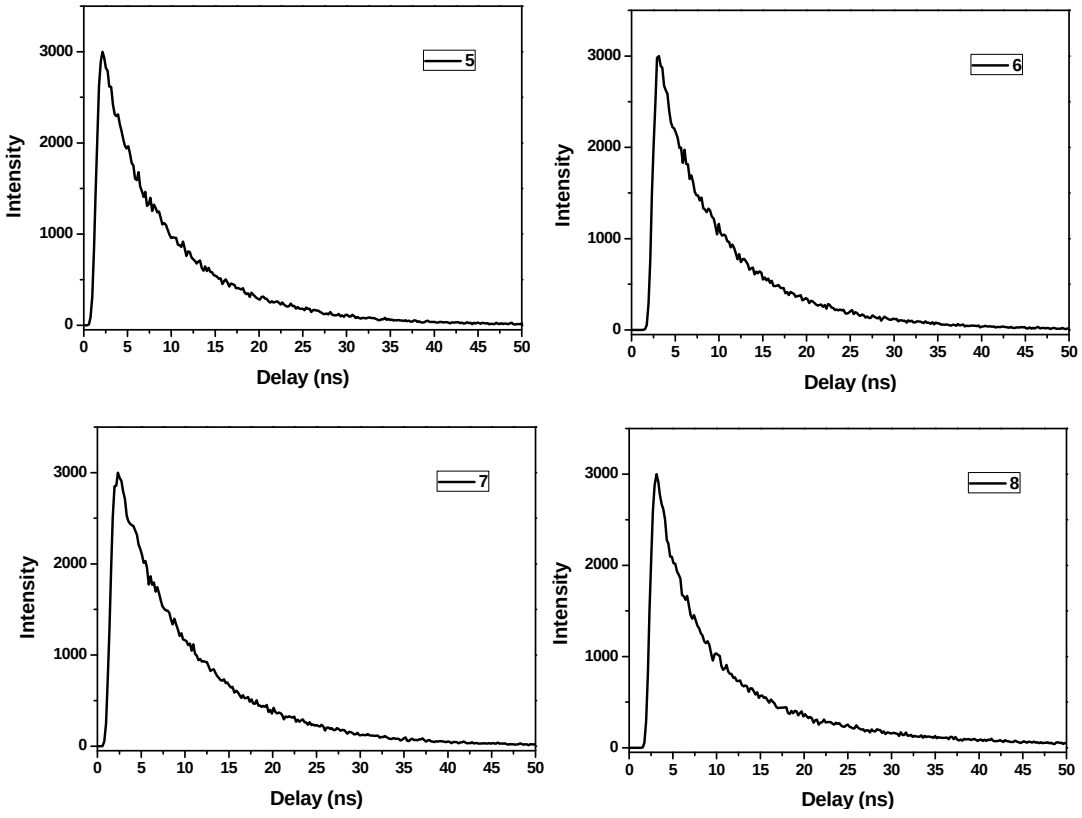

Figure S16. Fluorescence lifetime of **5-8** in the solid state (spin-coated film).

8. Photophysical data of 3 in solid state

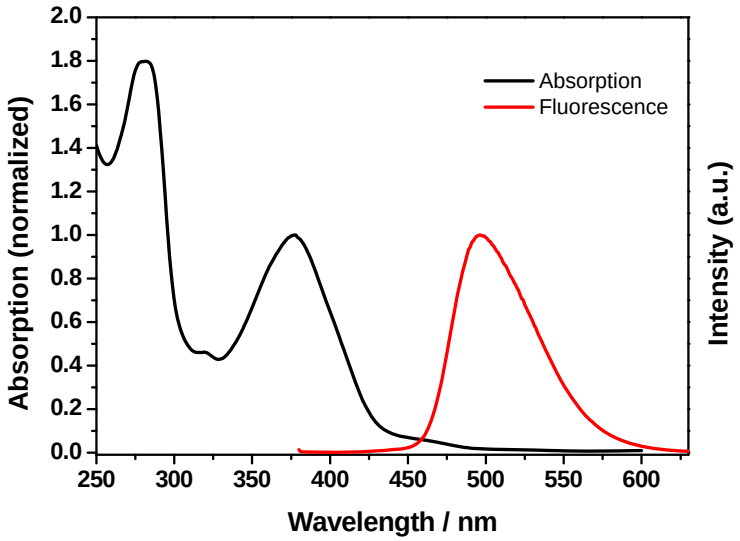

Figure S17. UV-Vis absorption and fluorescence spectra of **3** in the solid state (spin-coated film).

Table S10. Photophysical data of **3** in the solid state

Compound	λ_{abs}/nm	λ_{em}/nm	$\Phi_f{}^a$/%	τ/ns	Stokes shift /nm
3	377	496	25.5	10.56	119

[a]Absolute fluorescence quantum yield, measured by Hamamatsu Photonics Quantaurus QY

9. ^{1}H NMR and ^{13}C NMR spectra of new compounds

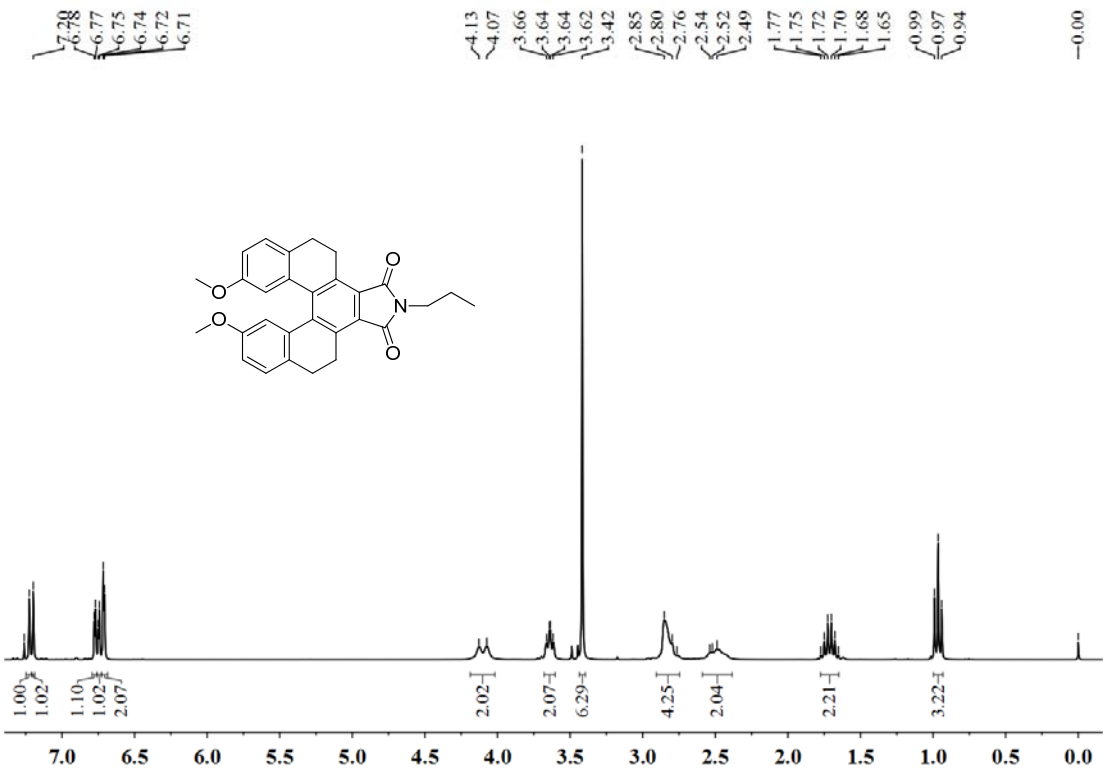

Figure S18. ^{1}H NMR spectrum (300 MHz, $CDCl_3$) of **3**.

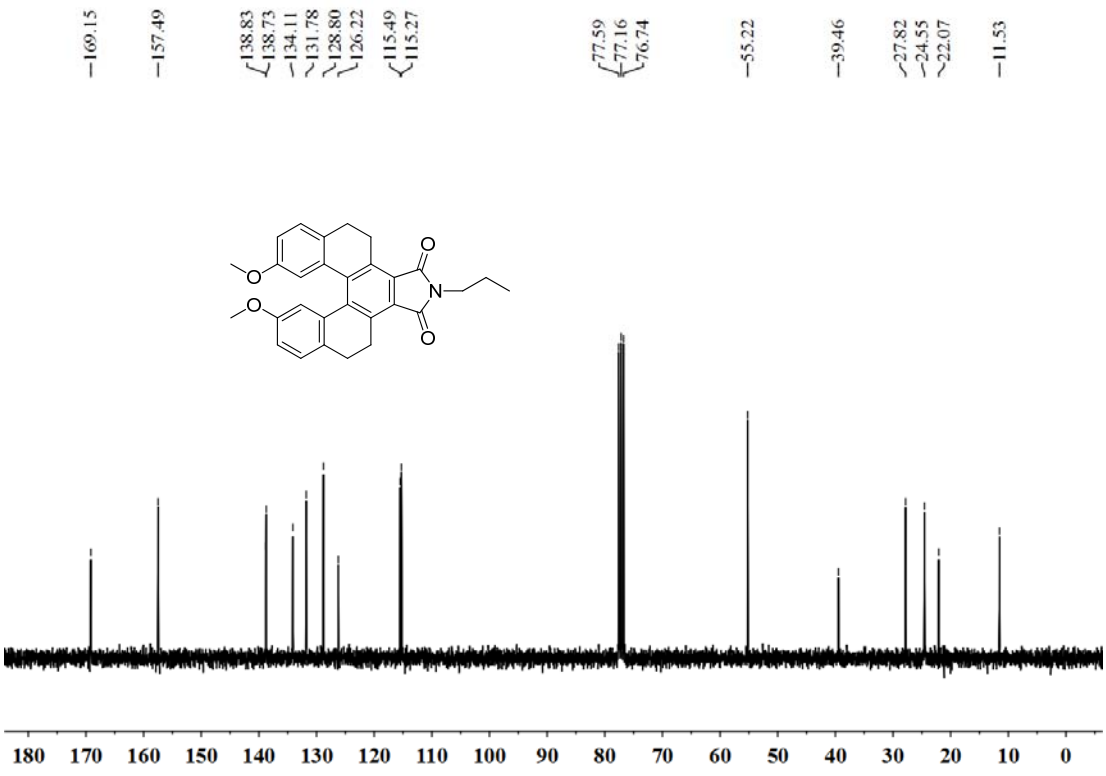

Figure S19. ^{13}C NMR spectrum (75 MHz, $CDCl_3$) of **3**.

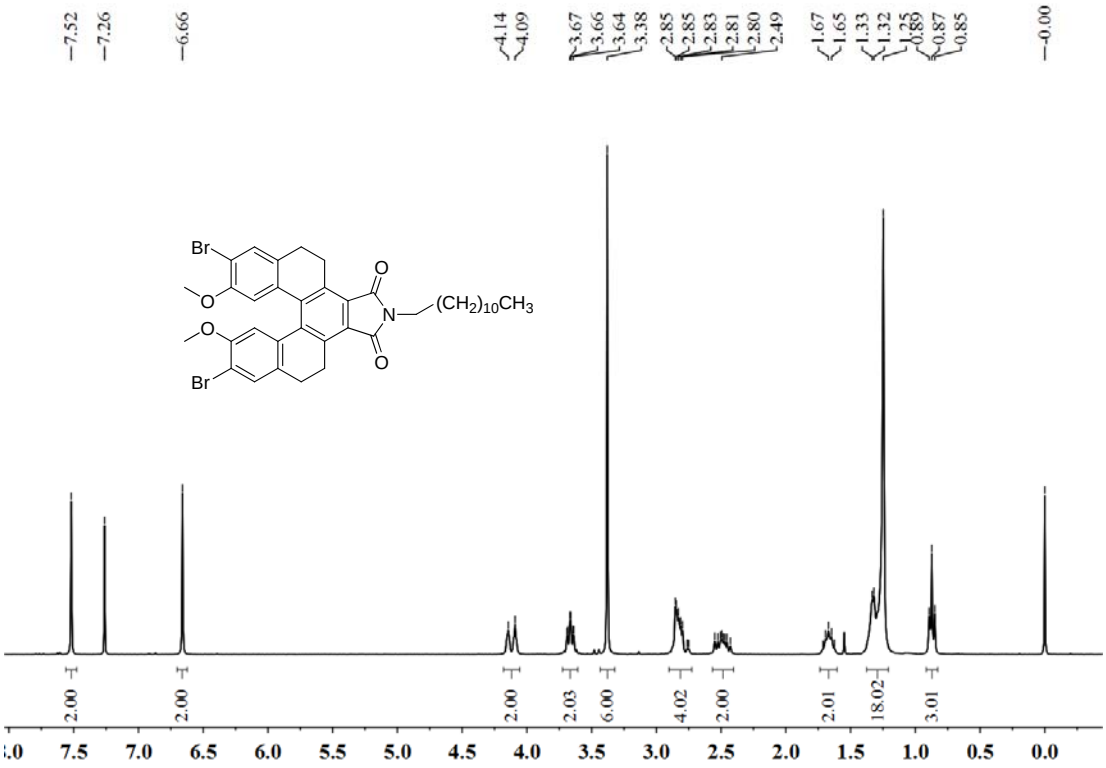

Figure S20. ^{1}H NMR spectrum (300 MHz, $CDCl_3$) of **4**.

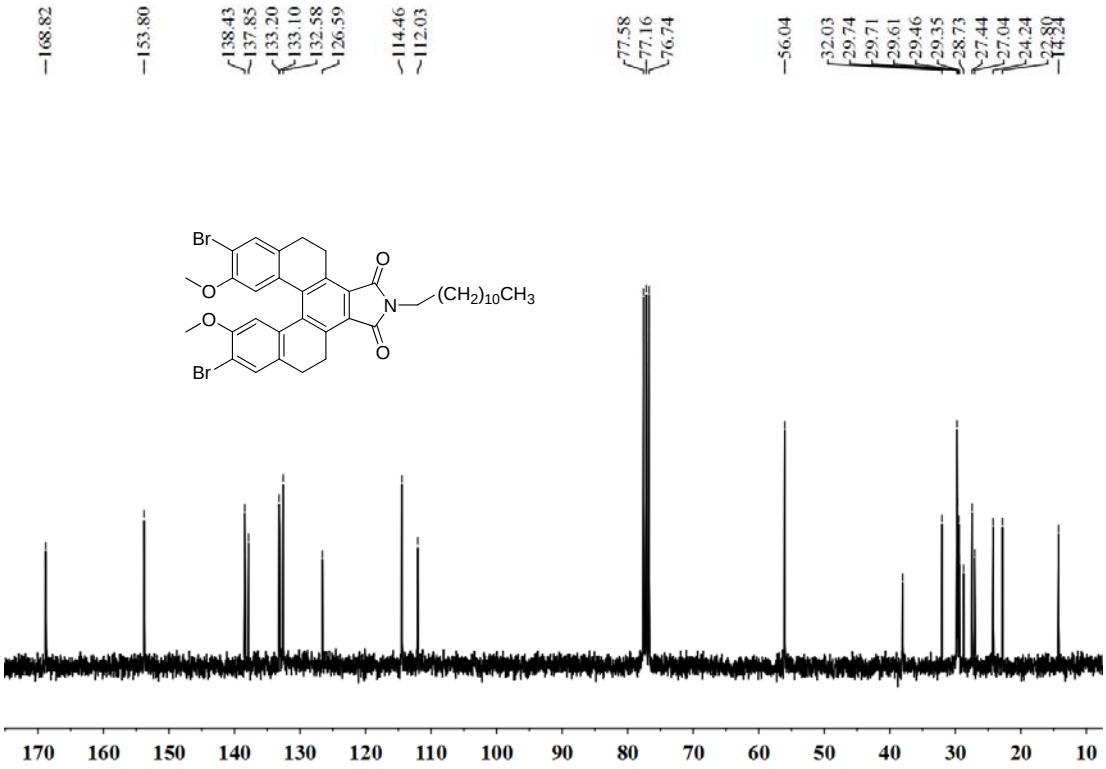

Figure S21. ^{13}C NMR spectrum (75 MHz, $CDCl_3$) of **4**.

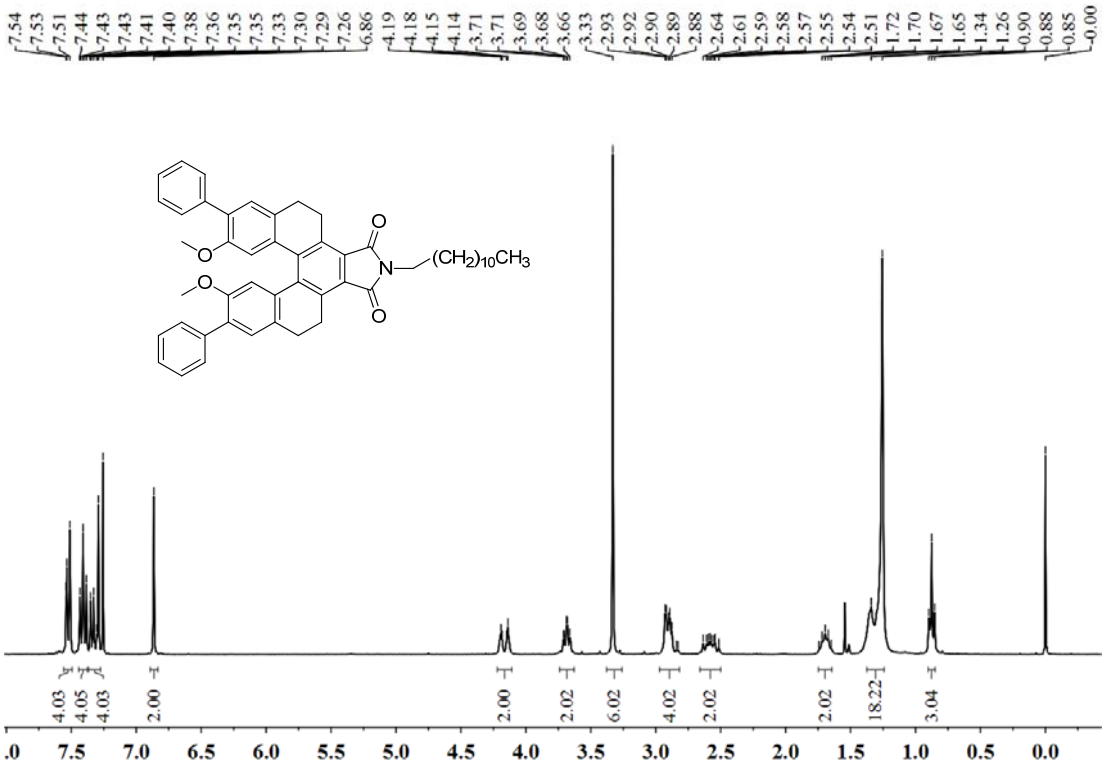

Figure S22. ^{1}H NMR spectrum (300 MHz, $CDCl_3$) of **5**.

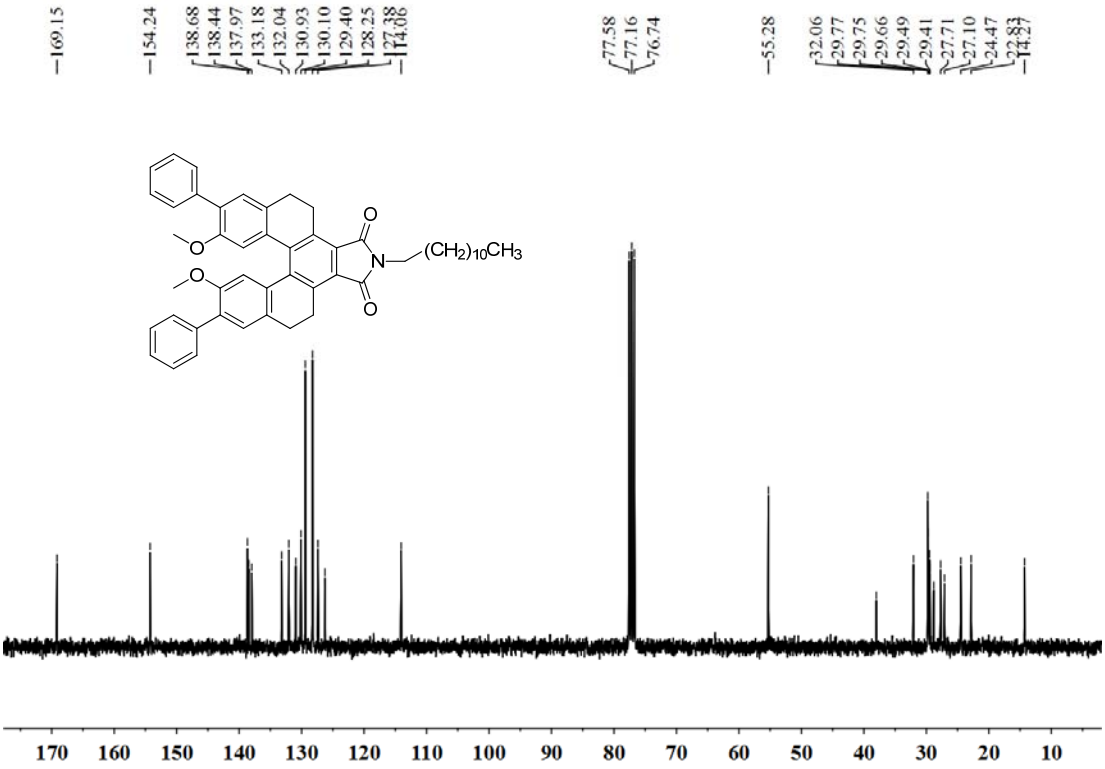

Figure S23. ^{13}C NMR spectrum (75 MHz, $CDCl_3$) of **5**.

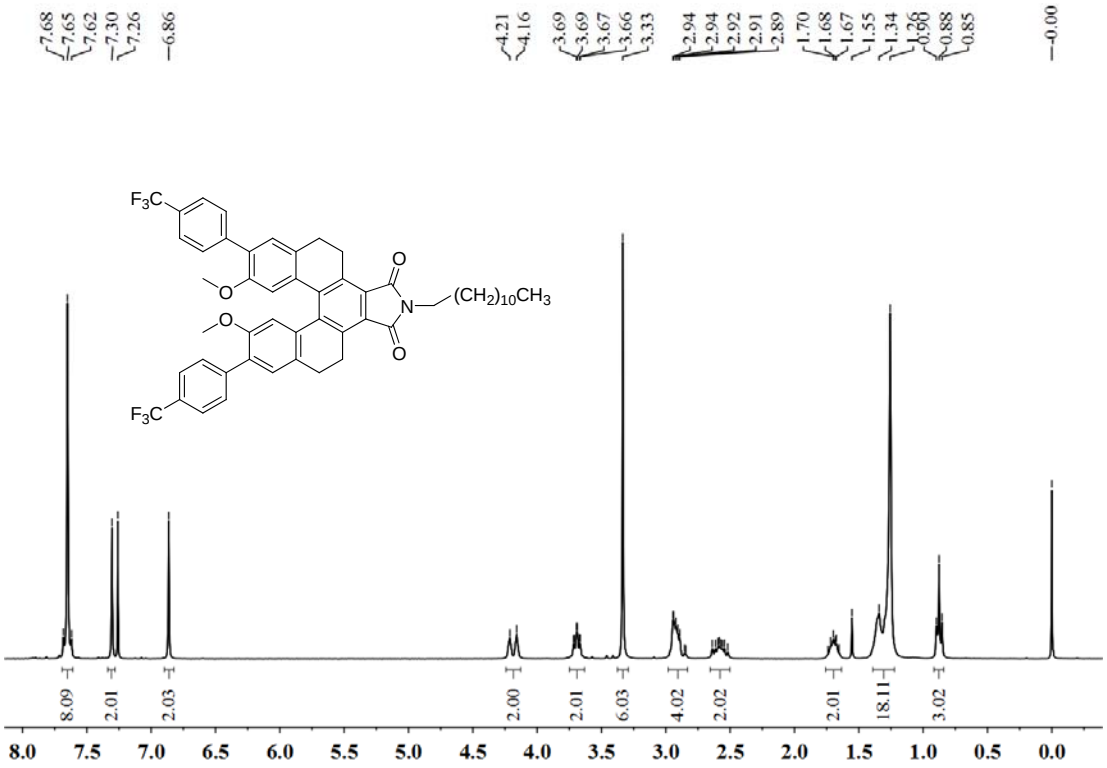

Figure S24. ^{1}H NMR spectrum (300 MHz, $CDCl_3$) of **6**.

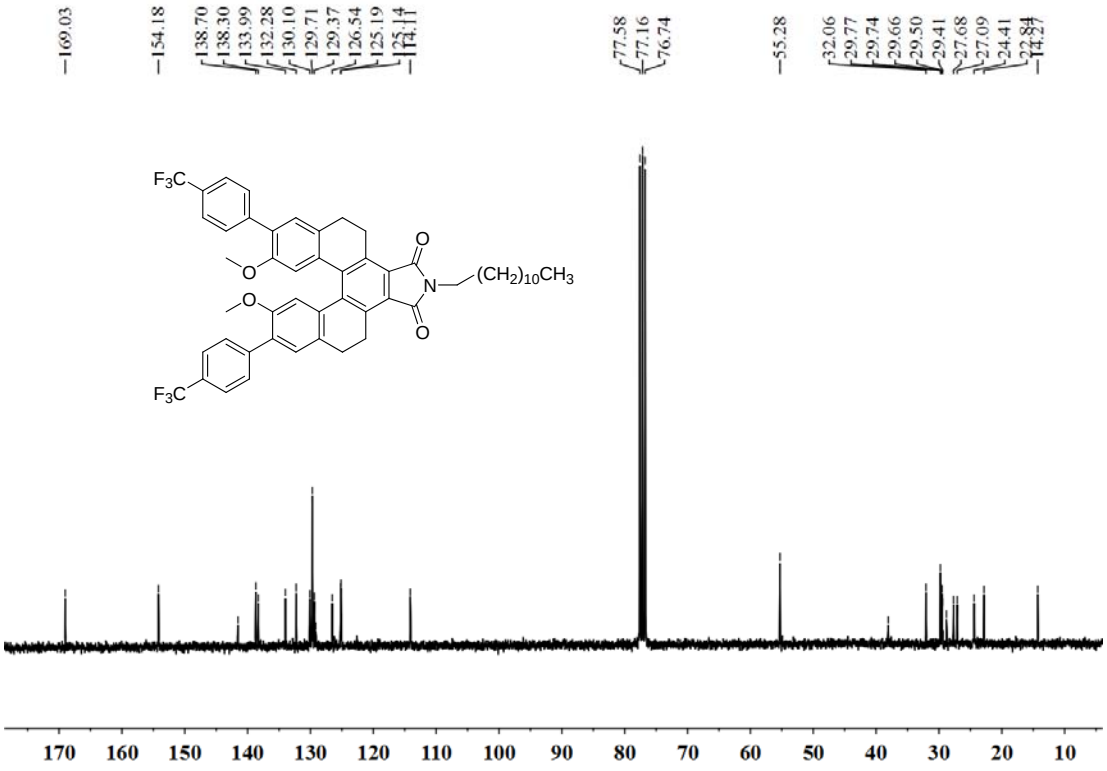

Figure S25. ^{13}C NMR spectrum (75 MHz, $CDCl_3$) of **6**.

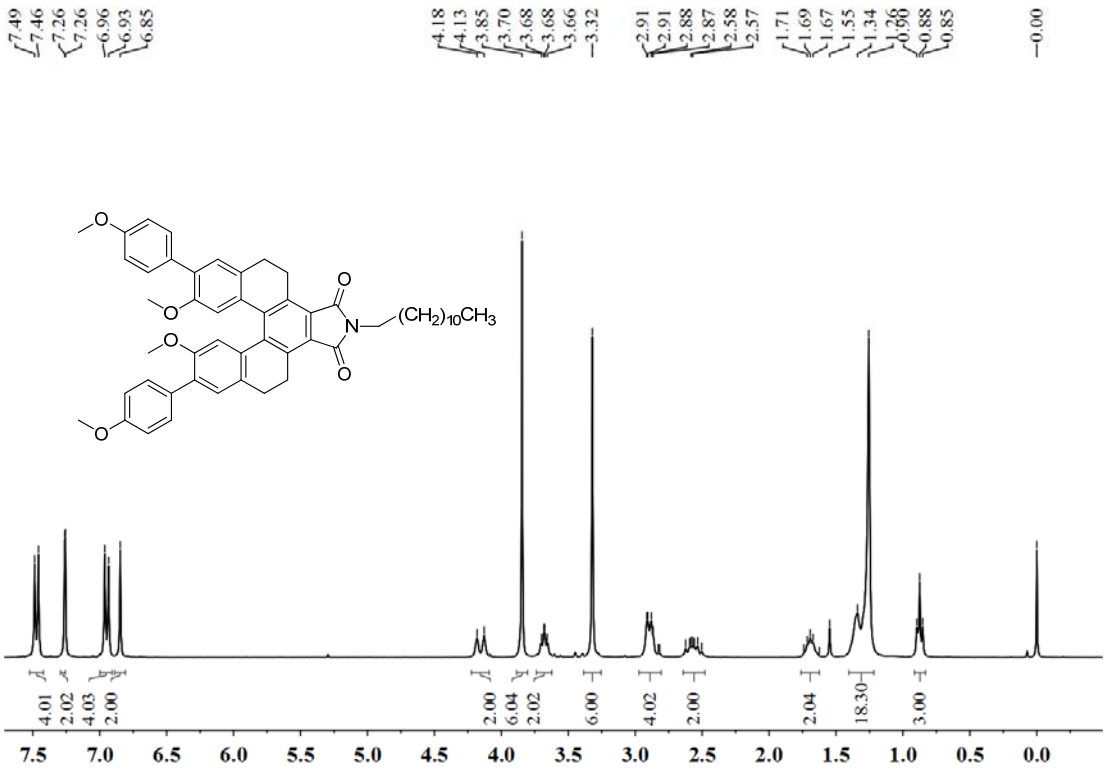

Figure S26. ^{1}H NMR spectrum (300 MHz, $CDCl_3$) of **7**.

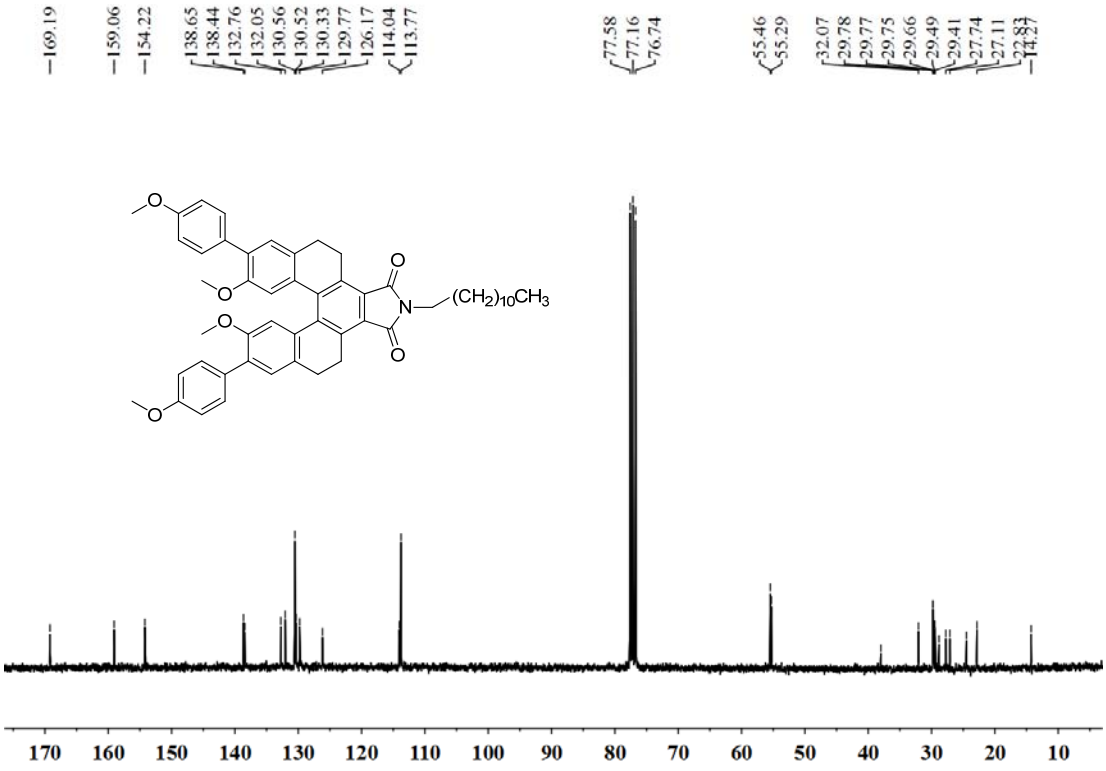

Figure S27. ^{13}C NMR spectrum (75 MHz, $CDCl_3$) of **7**.

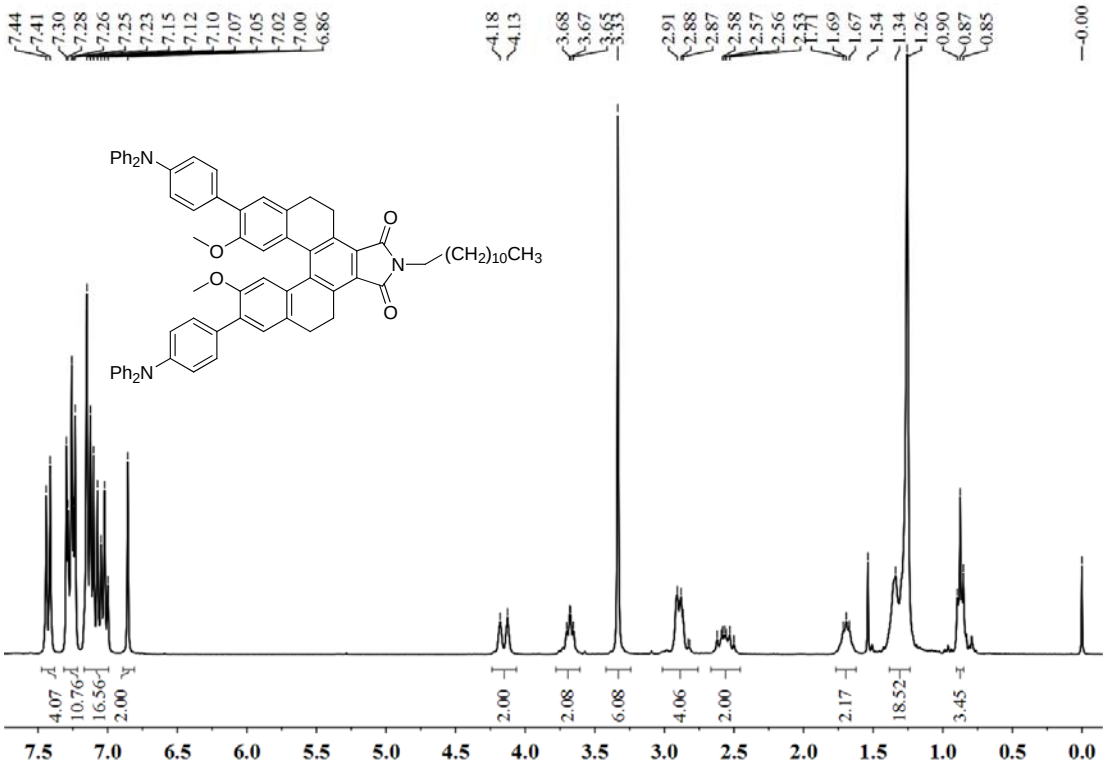

Figure S28. ^{1}H NMR spectrum (300MHz, $CDCl_3$) of **8**.

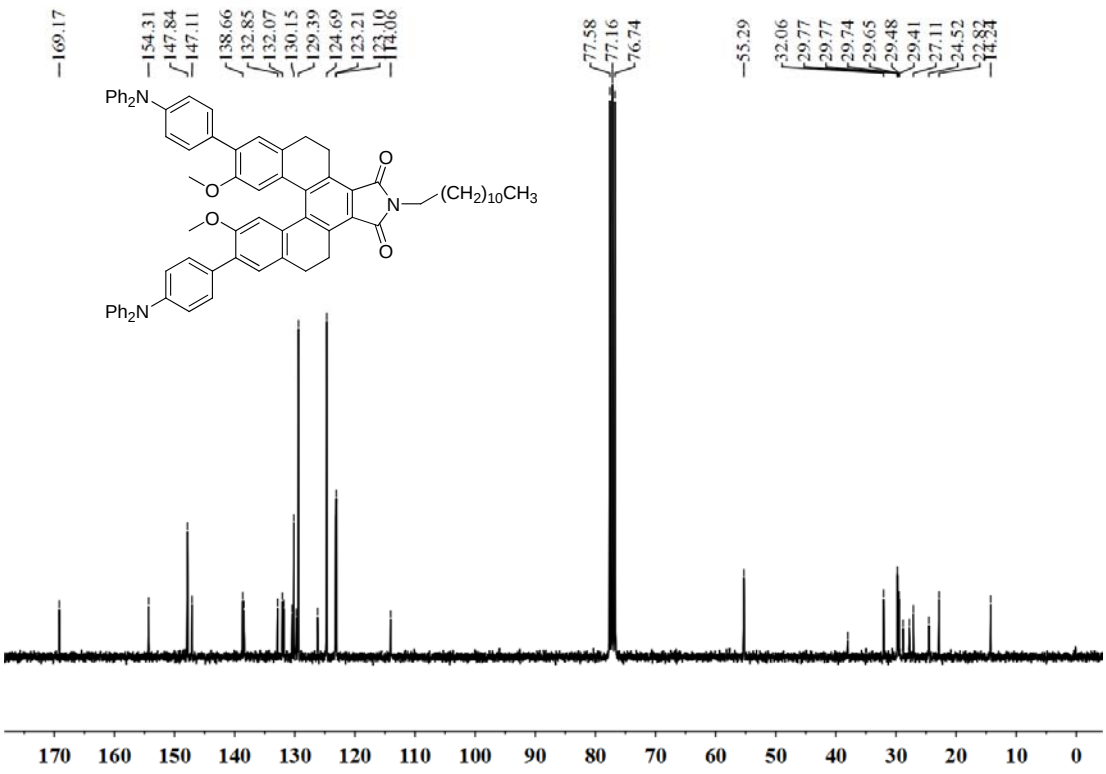

Figure S29. ^{13}C NMR spectrum (75 MHz, $CDCl_3$) of **8**.